JOC The Journal of Organic Chemistry

Article

pubs.acs.org/joc

A Taco Complex Derived from a Bis-Crown Ether Capable of Executing Molecular Logic Operation through Reversible Complexation

Amal Kumar Mandal, Priyadip Das, Prasenjit Mahato, Suhash Acharya, and Amitava Das*

CSIR-Central Salt and Marine Chemicals Research Institute, Bhavnagar, 364002, Gujarat, India

Supporting Information

ABSTRACT: As learned from natural systems, self-assembly and self-sorting help in interconnecting different molecular logic gates and thus achieve high-level logic functions. In this context, demonstration of important logic operations using changes in optical responses due to the formation of molecular assemblies is even more desirable for the construction of a molecular computer. Synthesis of an appropriate divalent as well as a luminescent crown ether based host **1** and paraquat derivatives, $\mathbf{2}(PF_6)_2$ and $\mathbf{3}(PF_6)_2$, as guests helped in demonstrating a reversible [3](taco complex) ($\mathbf{1}\cdot\{\mathbf{2}(PF_6)_2\}_2$ or $\mathbf{1}\cdot\{\mathbf{3}(PF_6)_2\}_2$) formation in nonpolar solvent. Detailed ^{1}H NMR studies revealed that two paraquat units were bound cooperatively by the two crown units in **1**. Because of preorganization, the flexible host molecule **1** adopts a folded conformation, where each of two paraquat units remain sandwiched between the two aromatic units of each folded crown ether moiety in **1**. Disassembly of the "taco" complex in the presence of KPF_6 and reassembly on subsequent addition of DB18C6 was initially demonstrated by ^{1}H NMR spectral studies, which were subsequently corroborated through luminescence spectral studies. Further, luminescence spectral responses as output signals with appropriate and two independent molecular inputs could be correlated to demonstrate basic logic operation like OR and YES gates, while the results of the three molecular inputs could be utilized to demonstrate important logic operation like an INHIBIT gate.

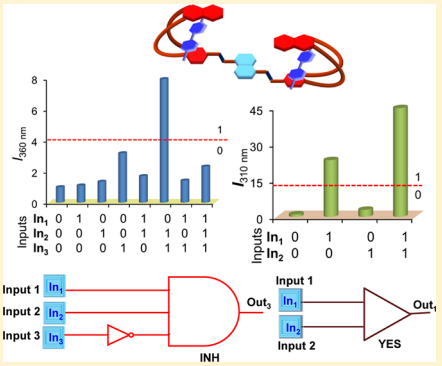

INTRODUCTION

In supramolecular chemistry, the controlled and reversible formation of molecular assemblies like rotaxanes/pseudorotaxanes or of taco complex formation between tailor-made host and guest component molecules along with changes in relative conformations of these individual components on formation of these assemblies are of enormous significance for the construction of molecular machines or developing information storage materials.[1] In this regard, design of the appropriate building block(s) having exciting properties for reversible formation of a predicted supramolecular assembly with desired conformation and property are crucial, as this allows switching between different assembled and disassembled states under the influence of various external stimuli. These designer assemblies have potential for use as organized molecular-scale devices, which are able to interpret, store, process, and dispatch information similar to the sophisticated machines found in natural systems. During the last three decades, recognition motifs based on crown ethers as host and organic cations, e.g., secondary dialkylammonium salts,[2] or paraquat derivatives,[3] as guest have played a significant role in demonstrating such possibilities. Paraquat derivatives (*N*,*N*′-dialkyl-4,4′-bipyridinium salts) are commonly being used as guest molecules in achieving such assemblies because of their easy availability, interesting physicochemical properties, and abilities to adopt different conformations (threaded or taco complex formation) based on the final conformation of the host component in these assemblies.[1a,4] Formation of such assemblies and changes in conformations of associated host and/or guest component(s) in most instances are primarily studied by ^{1}H NMR spectroscopy. Literature examples, wherein such processes are probed by monitoring changes in optical responses are very limited.[5] Further, examples of such supramolecular assembly wherein the reversible assembly and or disassembly process could be demonstrated as a function of external stimulation in the form of molecular input are rare.

Earlier, Stoddart and co-workers reported formation of pseudorotaxanes from paraquats and bisarylene crown ethers bearing 32−34 core atoms.[6] They have also shown that both a pseudorotaxane and an "exo" complex can form independently under different crystallization conditions for 1,5-bis((3,5-di-*tert*-butylbenzyl)ammonium)pentane bis(hexafluororophosphate) and bis(*p*-phenylene)-34-crown-10.[7] This suggests that both complexes can and possibly do exist in solution. More recently, Gibson et al. showed that complexation between bis(5-hydroxymethyl-1,3-phenylene)-32-crown-10 and paraquats derivatives led to an exo- or taco-complex formation,[8] which was influenced by the favorable $\pi-\pi$ stacking interaction(s) owing to the folded conformation of the flexible host molecule. They also reported the influence of counteranions on K_a during "taco" complexation of paraquat-based guest and crown ether

Received: March 31, 2012
Published: July 26, 2012

 © 2012 American Chemical Society dx.doi.org/10.1021/jo300622b | *J. Org. Chem.* 2012, 77, 6789−6800

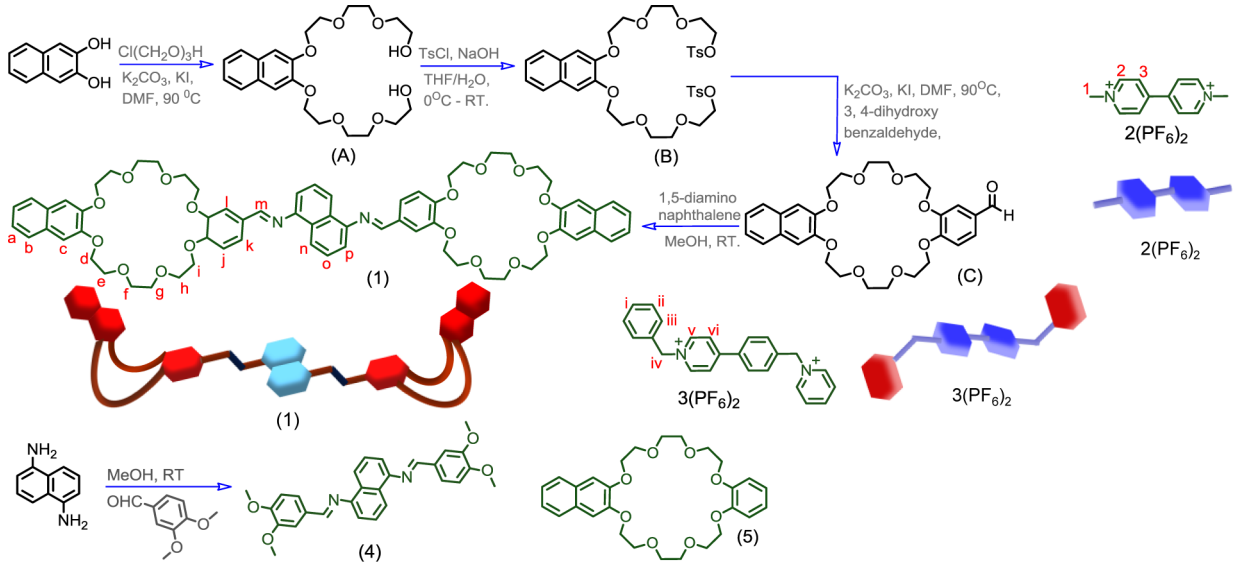

Figure 1. Schematic representation of the methodology that was adopted for synthesis of **1** and **4**, guest molecules ($\mathbf{2}(PF_6)_2$ and $\mathbf{3}(PF_6)_2$), and the model macrocyclic host **5**, which were used in this study.

based host molecules.[8b] It has been argued that the favorable entropy change that results from preorganization of the host molecule while adopting the folded state during the complexation processes influences the overall stability in such taco complexes.[9] Folding being an addressable step for the formation of such "taco" complexes, proper choice and introduction of substituents allows a smart control in improving the stability of such taco-complex and thereby a host–guest interactions.

In the macroscopic world, logic devices are incorporated in machines and devices for demonstrating desired logic functions. The challenge for the miniaturization problem faced by silicon-based electronics has actually led to the development of molecular logic gates as an emerging research area.[10] Since the first unambiguous demonstration of Boolean logic operation using a specified set of molecules and external stimulation in the form of molecular inputs by de Silva et al.,[11] numerous molecules capable of basic logic functions, like AND,[12] OR,[13] NAND,[14] INHIBIT,[15] NOR,[16] XOR,[17] and XNOR,[18] have been reported. Molecular combinatorial logic circuits, such as a digital adder,[19] subtractor,[20] comparator,[21] and multiplexer,[22] have also been realized. Although complex logic functions could be achieved or demonstrated by using a single molecule, realization of a true molecular computer is far from reality. Interconnection between different logic operations is required to create more complex logic circuits,[10b,23] and this still remains as a challenge for researchers active in this area. As learnt from natural systems, self-assembly[24] and self-sorting[25] may work as a glue to interconnect different molecular logic gates and thus achieve higher-level logic functions. Such an approach may open up the possibility of achieving higher logic operation(s) through appropriately designed molecular assemblies and by correlating different optical responses as a result of the formation of such assembly.[26]

In this contribution, we report the design and synthesis of divalent crown ether **1** having two photoactive naphthalene units as signaling fragments and two dibenzo-[24]-crown-8 ether moieties as the receptor fragments for two different parquat derivatives in nonpolar solvent. Detailed ^{1}H NMR studies reveal that two parquat units bind cooperatively with the crown ether-based host fragments in **1** to form eventually [3](taco complex). Because of preorganization of the flexible host molecule during binding, **1** adopts a folded conformation, wherein the paraquat-based guest component forms a sandwiched type assembly. Reversible formation, disassembly and reformation of the "taco" complex could be demonstrated using external molecular stimulations in the form of KPF_6 and dibenzo-18-crown-6 (DB18C6) and through ^{1}H NMR spectral studies. Achieving three states, namely, assembled, disassembled and reassembled by sequential addition of KPF_6 and DB18C6 could also be probed by monitoring distinct changes in luminescence spectra. By adopting appropriate threshold values and a logic convention, molecular input and output signals could be used to encode binary information.

Monitoring the observed fluorescence response at different wavelength, as output signals we obtained two basic gate OR and YES by using two inputs and an INHIBIT gate by using three inputs. To the best of our knowledge, demonstration of such logic operations using a self-assembled "exo" complex is extremely rare in the contemporary literature.

RESULTS AND DISCUSSION

Synthesis. Molecular structures and schematic representation of the bis-crown ether based host molecule **1**, two guest molecules as their hexafluorophosphate salt {$\mathbf{2}(PF_6)_2$ and $\mathbf{3}(PF_6)_2$}, along with two reference compounds **4** and **5** are shown in Figure 1. The 1,5-naphthalenediamine bridged divalent host **1** was synthesized in a convergent manner after four intermediate steps in a reasonable yield (80%). Two paraquat derivatives, $\mathbf{2}(PF_6)_2$ and $\mathbf{3}(PF_6)_2$, were synthesized by treating 4,4′-bipyridine with an excess of the appropriate alkyl halide in acetonitrile, and their desired hexafluorophosphate salts were isolated as insoluble solids by anion exchange in aqueous media. The other model compound **5**, along with intermediates A and B, were synthesized following previously reported procedures.[5a]

Complexation of Divalent Host 1 with $\mathbf{2}(PF_6)_2$ and $\mathbf{3}(PF_6)_2$. The divalent host **1** in $CDCl_3$:CD_3CN (4:1, v/v) solution was found to be light brown in color. However, this solution turned dark brown when 2 mol equiv of $\mathbf{2}(PF_6)_2$ were

dx.doi.org/10.1021/jo300622b | J. Org. Chem. 2012, 77, 6789–6800

added, and this change in color was due to the formation of a charge-transfer complex between the electron-rich aromatic rings of the host **1** and the electron-deficient bipyridinium rings of **2**$(PF_6)_2$. A Job's plot analysis (see Figure 4b) based on ^{1}H NMR data revealed that the stoichiometry for the host–guest complex was 1:2. This was confirmed by electrospray ionization mass spectrometry (ESI-MS) and MALDI-TOF mass data (Supporting Information Figures S2 and S4). In both mass spectral techniques, for a mixture of **1** and **2**$(PF_6)_2$ in the molar ratio of 1:2, the peak for $[\mathbf{1}\cdot\{\mathbf{2}(PF_6)_2\}_2 - PF_6]^+$ was observed at m/z 1983.6. The change in solution color on addition of benzyl derivative **3**$(PF_6)_2$ to **1** was not so prominent compared to that discussed above for **2**$(PF_6)_2$ under identical experimental condition; however, this gave the first evidence for the formation of a complex between **1** and **3**$(PF_6)_2$. A Job's plot analysis (see Figure 6b) based on ^{1}H NMR data demonstrated that the binding stoichiometry was 1:2 in $CDCl_3$:CD_3CN (4:1, v/v) solution. This was confirmed by ESI-MS and MALDI-TOF mass data (Supporting Information Figures S3 and S5). The peak for $[\mathbf{1}\cdot\{\mathbf{3}(PF_6)_2\}_2 - PF_6]^+$ was observed at m/z 2287.1 recorded using both techniques for a 1:2 mixture of **1** and **3**$(PF_6)_2$.

Let us first establish the complexation process for the formation of a 1:2 complex between **1** and **2**$(PF_6)_2$. The complexation of **1** and **2**$(PF_6)_2$ in $CDCl_3$:CD_3CN (4:1 v/v) solution was investigated in detail by ^{1}H NMR spectroscopy using different stoichiometric ratios by systematically varying the concentration of the guest fragment. Partial ^{1}H NMR spectra of **1**, **2**$(PF_6)_2$, and a mixture of **1** and **2**$(PF_6)_2$ are shown in Figure 2. Only one set of peaks was observed in the ^{1}H NMR

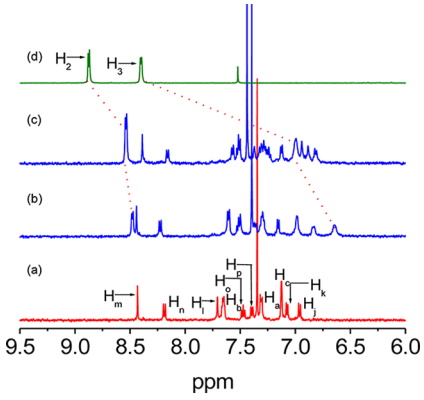

Figure 2. Partial ^{1}H NMR spectra (500 MHz, 298 K) recorded in $CDCl_3$:CD_3CN (4:1, v/v) for (a) 4.2 mM **1**, (b) 4.2 mM **1** with 4.2 mM **2**$(PF_6)_2$, (c) 4.2 mM **1** with 8.4 mM **2**$(PF_6)_2$, and (d) 8.4 mM **2**$(PF_6)_2$.

spectrum of the mixed solution of **1** and **2**$(PF_6)_2$, which implied that the equilibrium kinetics were fast within the ^{1}H NMR time scale at the 500 MHz frequency. After complexation, appreciable upfield shifts in signals corresponding to bipyridinium protons H_2 ($\Delta\delta$ = −0.34 ppm), H_3 ($\Delta\delta$ = −1.40 ppm) and the *N*-methyl protons H_1 ($\Delta\delta$ = −0.12 ppm) were observed, which suggested that these paraquat protons resided under the shielding influence of the aromatic rings of the host molecule **1** during binding. Chemical shifts for two sets of aromatic protons of the divalent host were quite interesting. Significant upfield shifts for aromatic protons (H_a, H_b and H_c) of the terminal naphthalene unit and the protons of the phenyl ring (H_j ($\Delta\delta$ = −0.33 ppm), H_k ($\Delta\delta$ = −0.14 ppm), and H_l ($\Delta\delta$ = −0.16 ppm)) were observed, which revealed that these aromatic rings were also under the shielding influences of the bipyridinium rings. Shifts of the aromatic protons of the central naphthalene unit were rather different.

A gradual but small downfield shift ($\Delta\delta$ = 0.04 ppm) for the H_o proton was observed on inclusion complex formation. Two other protons H_n and H_p as well as the imine proton (H_m) initially moved downfield, and then their position remained unchanged as the titration progressed. These observations were consistent with the proposed sandwich type complex formation (Figure 3). Possible conformation for the host–guest complex

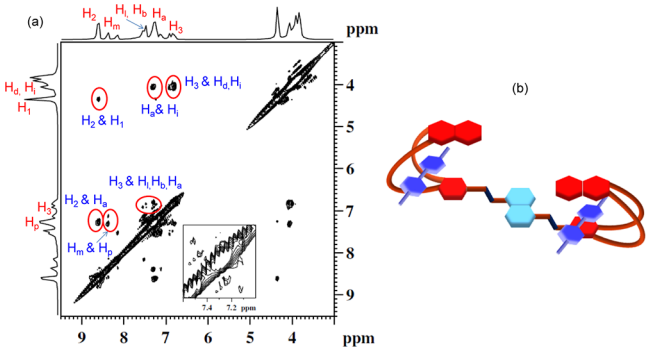

Figure 3. (a) Partial 2D-NOESY spectrum (500 MHz, 298 K) recorded for 4.2 mM **1** with 8.4 mM **2**$(PF_6)_2$ in $CDCl_3$:CD_3CN (4:1, v/v). (b) Schematic representation of the mode of binding of **1** and **2**$(PF_6)_2$ due to formation of a [3](taco complex).

(Figure 3) suggests that central naphthalene ring and the imine protons are not within the shielding influence of the aromatic rings of the paraquat guest and formation of an inclusion complex with cationic guest component accounts for their small but definite downfield shifts. All the ethyleneoxy protons of the crown ether were upfield shifted on complexation, and shifts were most significant for H_d and H_i ($\Delta\delta$ = −0.21 ppm).

To gain more insight into the complexation process and the relative orientation of the individual host and guest components in the inclusion complex, we performed 2D-NMR studies. The 2D-NOESY spectrum of **1** in presence of 2 mol equiv of **2**$(PF_6)_2$ was recorded in $CDCl_3$:CD_3CN (4:1 v/v) at room temperature and is shown in Figure 3a. Strong correlations between the bipyridinium proton H_3 and the ethyleneoxy protons (H_d and H_i) of the crown unit indicates that these two sets of protons come closer to the bipyridinium units during binding. Two sets of cross peaks were also observed for the interaction of H_3 with H_a and H_b of the terminal naphthalene unit as well as H_l of the phenyl unit of the divalent host. These results suggest that the terminal naphthalene unit and the phenyl unit are in a position after binding, where they interact simultaneously with the bipyridinium units. The cross peak was also observed for the interaction of H_2 of the bipyridinium unit and H_a of the terminal naphthalene unit. A correlation between the H_m and H_p proton in the 2D-NOESY spectrum also suggests that the central aromatic units of the divalent host remains planar while it forms the host–guest complex. The cross peaks in the 2D-COSY spectrum of **1** in the presence of 2 mol equiv of **2**$(PF_6)_2$ were recorded in $CDCl_3$:CD_3CN (4:1, v/v) at room temperature, which also supported the formation of the host–guest adduct (Supporting Information Figure S6).

Previous literature reports on inclusion complex formation between crown ether derivatives and paraquat units suggest two

dx.doi.org/10.1021/jo300622b | J. Org. Chem. 2012, 77, 6789–6800

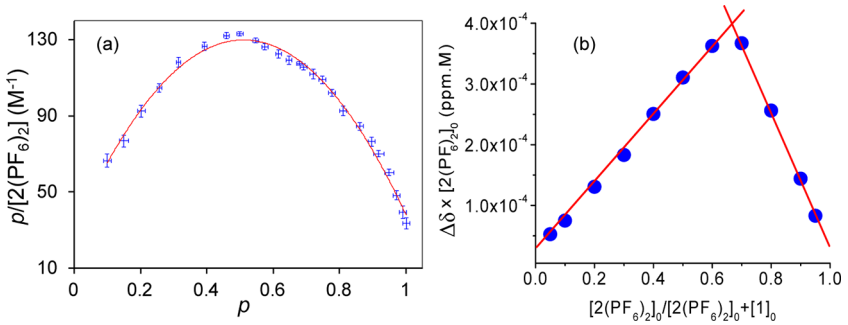

Figure 4. (a) Scatchard plot for the complexation of **1** ($[\mathbf{1}]_0 = 4.2 \times 10^{-3}$ M) with $\mathbf{2}(PF_6)_2$ in $CDCl_3$:CD_3CN (4:1, v/v) at 25 °C ($y = -383.34x^2 + 391.48x + 29.88$, $R^2 = 0.99$), where p is fraction of **1** units bound. Error bars in p: ± 0.01; error bars in $p/\mathbf{2}(PF_6)_2$: ± 3.06. (b) Job's plot that reveals a 1:2 binding stoichiometry between **1** and $\mathbf{2}(PF_6)_2$ in $CDCl_3$:CD_3CN (4:1, v/v) using changes in chemical shift (δ) data for H_d, while $[\mathbf{1}]_0 + [\mathbf{2}(PF_6)_2]_0 = 7.3 \times 10^{-3}$ M.

possible modes of binding during complexation;[6−9] either formation of a pseudorotaxane type interwoven complex takes place wherein the paraquat ion is threaded through the macrocyclic host or formation of a "taco" complex wherein the guest is sandwiched within the aromatic units of the folded host. Mainly three possible binding interactions, e.g., hydrogen bonding, face-to-face π-stacking, and $N^+\cdots O$ ion dipole interactions, are expected to contribute to the stability of the adduct. The most prominent binding interactions are hydrogen bonding between O_{Crown} and acidic hydrogens of the paraquat unit and $\pi-\pi$ stacking interactions between the electron poor pyridinium ring and aryl units of the crown ether-based host. Gibson et al. reported a [3](taco complex) from a linear bis(crown ether) as host and paraquat ion as guest; taco complex formation was confirmed by ^{1}H NMR spectra as well as by single crystal X-ray structure.[27] They also reported a capsular structure that results from an opposing, head-to-head orientation of the two DB24C8, wherein the benzene rings $\pi-\pi$ stack with the pyridinium units of the paraquat guest.[28] However, a report on analogous complex formation by Stoddart et al. with the diazapyrenium salt features a head-to-tail structure of the two host species in which one pair of benzo rings does not interact with the guest.[29] A recent report by Chen et al. reveals that a triptycene-based cylindrical macrotricyclic polyether containing dibenzo-24-crown-8 cavities form "taco" complex with different functional paraquat derivatives.[30] Comparison of the literature reports and results of our ^{1}H NMR experiments discussed above led us to conclude that a [3]taco complex involving **1** and two molecules of $\mathbf{2}(PF_6)_2$ probably has the conformation shown in Figure 3b. The flexibility of the crown ether in solution is expected to allow rapid folding such that the phenyl rings and the terminal naphthalene ring interact with pyridinium rings of the guest to adopt a folded [3](taco complex) conformation.

In order to study the relationship between the two crown ether binding sites during formation of the [3](taco complex), ^{1}H NMR spectra were recorded for a series of $CDCl_3$:CD_3CN (4:1, v/v) solutions of **1** (4.2 mM) with systematic variation of $[\mathbf{2}(PF_6)_2]$. On the basis of these ^{1}H NMR data, the extent of complexation, p (Supporting Information page 4), of the crown ether units was determined and a Scatchard plot was made (Figure 4a). The nonlinear nature of this plot with a maximum demonstrated that positive cooperativity had driven the complex formation processes.[31]

Analysis of the Scatchard plot enabled us to find out the stoichiometric binding constants K_1 and K_2 and also the apparent average association constant (K_{av}). To find out the stoichiometric binding constants, the following equations were used: $K_1 = [\mathbf{1}\cdot\mathbf{2}(PF_6)_2]/\{[\mathbf{1}]\cdot[\mathbf{2}(PF_6)_2]\}$ and $K_2 = [\mathbf{1}\cdot\{\mathbf{2}(PF_6)_2\}_2]/\{[\mathbf{1}\cdot\mathbf{2}(PF_6)_2]\cdot[\mathbf{2}(PF_6)_2]\}$. The slope of the first six data points for low p (Figure 4a) gave the value of $(2K_2 - K_1)$, while the slope of the last 10 data points for high p (Figure 4a) gave the value of $-2K_2$.[31f] Thus, the value for K_1 was found to be 1.0 (±4.4) × 10^2 M^{-1}, while that for K_2 was 1.6 (±0.4) × 10^2 M^{-1}. The ratio $K_2/K_1 = 1.6$ is significantly higher than the value of 0.25 that is expected for statistical complexation[31b,g] and supports the cooperative nature of binding. Formation of the 1:1 complex is expected to effectively restrict conformational changes of crown moiety due to the hydrogen bonding interactions between the paraquat protons with crown ether oxygen atoms, and this conformational restriction presumably facilitates complexation of the second crown ether site and accounts for the apparent observed cooperativity. As mentioned by Hayman,[31b] in case of positive cooperativity it is misleading to say that the first ligand is bound less strongly than the subsequent ligands. Rather, positive cooperativity means that in the bis-complex both ligands are bound more strongly than the first ligand is in the monocomplex. In the present study, the apparent average association constant was found to be $K_{av} = (K_1 + K_2)/2 = 1.3$ (±1.6) × 10^2 M^{-1}, which is bigger than that reported for 2:1 complex formation between dibenzo-[24]-crown-8 and the paraquat.[28] But the apparent average association constant is lower than the association constant value of 3.7 (±0.4) × 10^2 M^{-1} reported for paraquat-based [3](taco complex) prepared from a linear bis-crown ether-based host having bis(*m*-phenylene)-32-crown-10 as binding motif.[27] The average binding constant, evaluated for the present study, is also lower than the value reported by Chen et al., 4.0 × 10^3 M^{-1} for a triptycene paraquat based [2](taco complex) having dibenzo-[24]-crown-8 as the host.[30b] It may be mentioned here that we have ignored the possibility of the ion pairing of paraquat ion while computing the binding constant. The observed lower value of the binding constant in the present study is understandable, as the stability of "taco" complex depends on different parameters like the flexibility of the crown unit and the nature of substituent on the aromatic moiety.[8,9] Other factors like steric and conformational effects caused by the introduction of a substituent on the crown ether moieties are also expected to influence the overall binding constant.

Formation of the complex between **1** and $\mathbf{3}(PF_6)_2$ in $CDCl_3$:CD_3CN (4:1, v/v) was also studied in detail using ^{1}H

dx.doi.org/10.1021/jo300622b | J. Org. Chem. 2012, 77, 6789−6800

NMR spectroscopic studies. Only one set of peaks was observed in the ^{1}H NMR spectrum, which revealed fast exchange at 500 MHz.

Partial ^{1}H NMR spectra of **1**, **3**$(PF_6)_2$, and a mixture of **1** and **3**$(PF_6)_2$, are shown in Figure 5. As observed in case of **2**$(PF_6)_2$,

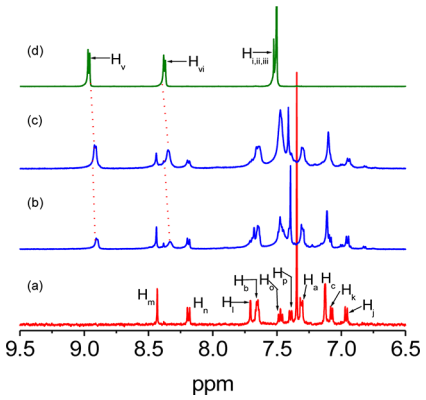

Figure 5. Partial ^{1}H NMR spectra (500 MHz, 298 K) recorded in $CDCl_3$:CD_3CN (4:1, v/v) for (a) 4.2 mM **1**, (b) 4.2 mM **1** with 4.2 mM **3**$(PF_6)_2$, (c) 4.2 mM **1** with 8.4 mM **3**$(PF_6)_2$, and (d) 8.4 mM **3**$(PF_6)_2$.

all bipyridinium protons (H_v and H_{vi}) including the *N*-methyelene (H_{iv}) and phenyl protons ($H_{i,ii,iii}$) were shifted upfield on formation of the host–guest complex. Though the extent of shifts observed was less compared to that of previous one, a similar shift pattern was observed for the protons of divalent host **1** after complexation. Cross peaks that were observed in the 2D-NOESY and COSY spectrum also confirmed the complex formation between **1** and **3**$(PF_6)_2$ in mixed solvent medium (Supporting Information Figure S7).

To study the relationship between the two crown ether binding sites of **1** during the complexation with **3**$(PF_6)_2$, ^{1}H NMR spectra were recorded for a series of solutions with a fixed concentration for **1** and varying concentration of **3**$(PF_6)_2$. On the basis of these data, the extent of complexation, p, of the crown ether units was determined and a Scatchard plot was drawn (Figure 6a). The nonlinear nature of this plot with a maximum confirmed positive cooperativity in the complex formation process.[31] The slope of the first six data points for low p (Figure 6a) gave the value of $2K_2 - K_1$, while the slope of the last 13 data points for high p (Figure 6a) gave the value of

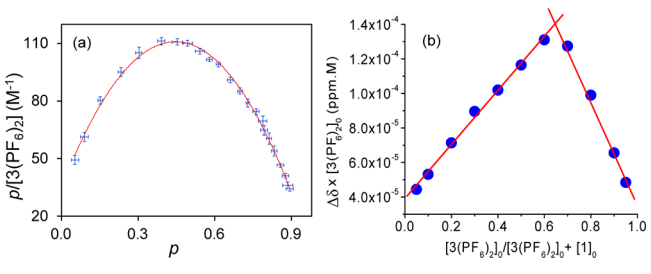

Figure 6. (a) Scatchard plot for the complexation of **1** ($[\mathbf{1}]_0 = 4.2 \times 10^{-3}$ M) with **3**$(PF_6)_2$ in $CDCl_3$:CD_3CN (4:1, v/v) at 25 °C ($y = -380.71x^2 + 354.69x + 28.16$, $R^2 = 0.99$), where p is fraction of **1** units bound. Error bars in p: ± 0.01; error bars in $p/[\mathbf{3}(PF_6)_2]$: ± 2.63. (b) Job's plot that reveals a 1:2 binding stoichiometry between **1** and **3**$(PF_6)_2$ in $CDCl_3$:CD_3CN (4:1, v/v) using changes in chemical shift (δ) data for H_d, while $[\mathbf{1}]_0 + [\mathbf{3}(PF_6)_2]_0 = 7.3 \times 10^{-3}$ M.

$-2K_2$. Thus, the value for K_1 was found to be 0.5 (±9.0) × 10^2 M^{-1}, and K_2 was 1.2 (±5.8) × 10^2 M^{-1}. Any possibility of ion paring of this paraquat derivative was also ignored. Thus the apparent average association constant was found to be $K_{av} = (K_1 + K_2)/2 = 0.8$ (±1.8) × 10^2 M^{-1}, which is lower than that we observed earlier for **2**$(PF_6)_2$. Presumably, the presence of benzyl units accounts for the lower formation constant for **1**·**3**$(PF_6)_2$.

Photophysical Study. An overview of the steady state spectroscopic data measured in air equilibrated CH_2Cl_2 solutions at room temparature is given in Table 1. The

Table 1. Spectroscopic Data Recorded for Compounds 1, 2$(PF_6)_2$, 3$(PF_6)_2$ and Respective Complexes 1·{2$(PF_6)_2$}$_2$ and 1·{3$(PF_6)_2$}$_2$ in CH_2Cl_2 Solution at Room Temperature

host/guest	$\varepsilon \times 10^{-3}$ (L mol^{-1} cm^{-1})	λ_{abs} (nm)	λ_{emi} (nm)	Φ (%)
1	26.9	280	342, 420	1.5
	19.9	365		
2$(PF_6)_2$	7.3	260	342	17.6
3$(PF_6)_2$	10.9	260	287	0.5
1·{**2**$(PF_6)_2$}$_2$	46.0	280	342	5.9
	21.4	373		
1·{**3**$(PF_6)_2$}$_2$	35.4	280	342	1.0
	20.3	365		
4	11.1	365	374	
5	9.2	280	320	

absorption spectrum of **1** mainly showed two band maxima at 280 nm and a broad band at 365 nm (Table 1), which could be attributed to electronic transitions associated with two different photoactive moieties, **D1** and **D2** (Scheme 1). To understand

Scheme 1. Schematic Drawing of 1 Indicating Two Different Units D1 and D2

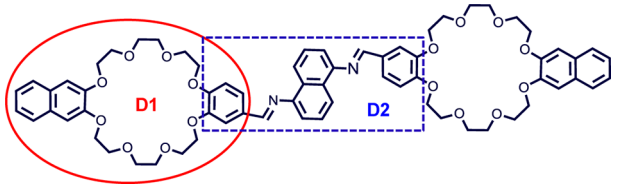

the nature of these electronic transitions better, two new reference compounds (**4** and **5**) were also synthesized, and their spectroscopic and physicochemical properties were measured for comparison. The absorption band at 280 nm for **5** was attributed to a naphthalene-based π–π^* transition, and for **4**, the broad band at 365 nm was ascribed to an intracomponent charge transfer (CT) band. Thus, a comparison of absorption spectra of **1** with that of **4** and **5** suggests that the broad band at 365 nm is due to the charge transfer transition of **D2** unit, while the other higher energy band at 280 nm is associated with the napthalene-based transition of **D1** unit (Scheme 1). Absorption spectra for **1** were also recorded in the presence of 2 equiv of **2**$(PF_6)_2$ or **3**$(PF_6)_2$. Interestingly on addition of **2**$(PF_6)_2$, a red shift of 8 nm for the charge transfer band (λ_{max} = 365 nm for **1**) was observed, and the broadness of the band was also enhanced. A similar trend in the spectral change was also observed when spectra for **1** were recorded in presence of 2 mol equiv of **3**$(PF_6)_2$, although the extent of change was less (Table 1) compared to spectra recorded in the presence of comparable concentrations of

dx.doi.org/10.1021/jo300622b | J. Org. Chem. 2012, 77, 6789–6800

Scheme 2. Relative Energies for the HOMO and LUMO Levels for 1, 4 and 5, 1·{2(PF$_6$)$_2$}$_2$ and 1·{3(PF$_6$)$_2$}$_2$, Which Were Evaluated from Respective Ground State Redox Potentials and E_{0-0} Values

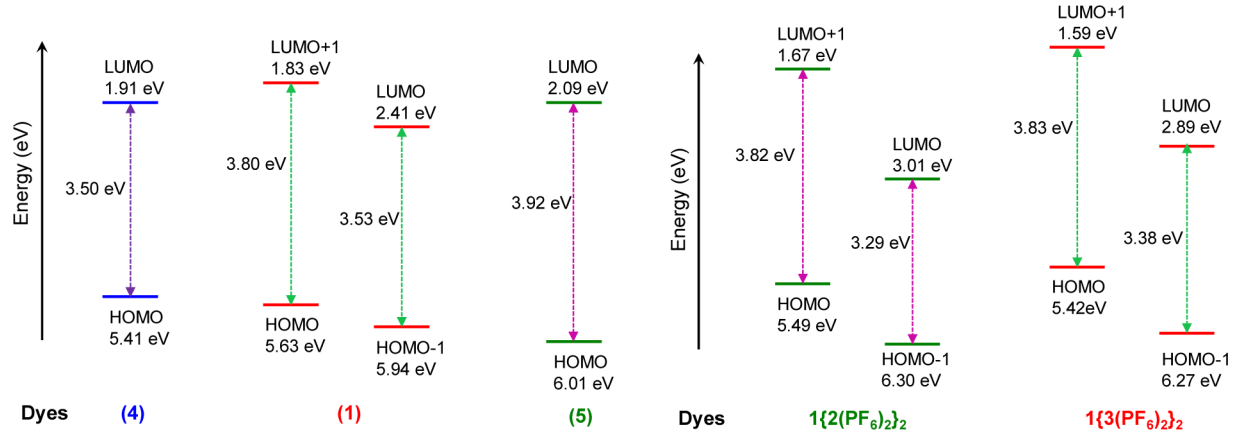

2(PF$_6$)$_2$. However, in both cases, features are indicative of the new charge transfer complex formation in the ground state in presence of 2 equiv of **2**(PF$_6$)$_2$ or **3**(PF$_6$)$_2$.

The emission spectrum of **1** in CH_2Cl_2 solution was recorded following excitation at 280 and 365 nm. On exciting at 280 nm, **1** showed two different emission bands with maxima at 342 and 420 nm, while one emission band with maxima at 420 nm was observed when λ_{Ext} of 365 nm was used. The weak emission of **1** (Φ = 0.0147) was attributed to the flexible nature of the crown moiety and the presence of lower energy ICT state.[32] **2**(PF$_6$)$_2$ exhibited a strong emission band (λ_{Ext} = 260 nm, Φ = 0.1762) with a maximum at 342 nm. The significant decrease of fluorescence quantum yield (Φ = 0.0593) observed for 1:2 mixture of **1** and **2**(PF$_6$)$_2$ also supports the formation of a CT complex. But the emission spectra of **1** in presence of 2 equiv of **3**(PF$_6$)$_2$ was a little different, and an overall decrease in emission quantum yield supports the CT complex formation (Table 1).

To obtain a better understanding about the relative energies of the frontier molecular orbitals, cyclic voltammetry (CV) studies were carried out for measuring the oxidation/reduction potential of the respective host−guest system. The results of the cyclic voltametric studies are provided in Table 3, and the respective energy levels associated with host and guest components are shown in Scheme 2.

Two oxidation potentials (E_{ox}) for **1**, corresponding to the highest occupied molecular orbital (HOMO) and (HOMO − 1) levels, were recorded. Two band gap energy (E_{0-0}) values for **1** were obtained from the intersection of the normalized absorption and emission spectra and were assigned to **D1** (HOMO to LUMO + 1 transition) and **D2** (HOMO − 1 to LUMO transition) based transitions, respectively (Supporting Information page 15). Interestingly, the E_{0-0} value of the **D1** unit was lower (0.12 eV) compared to the reference compound **5**. On the other hand, the E_{0-0} value that was assigned for **D2** unit almost remains unchanged (0.03 eV). This signifies a little alteration of the charge transfer state of the compound **4** due to the attachment of an additional moiety **D1**. Thus, these results indicate the presence of an intramolecular charge transfer state (ICT) in **1**. The results also suggest that the absorption bands of **1** at 280 and 365 nm could be ascribed to (HOMO to LUMO + 1) and (HOMO − 1 to LUMO) transitions, respectively. Similarly, the emission bands of **1** at 342 and 420 nm originated from LUMO + 1 to HOMO and LUMO to HOMO − 1 based transitions, respectively. Further, to get a better understanding about electronic and fluorescence spectral results, we also calculated the energy levels of the two different charge transfer complexes of **1** formed in presence of 2 equiv of either **2**(PF$_6$)$_2$ or **3**(PF$_6$)$_2$. In the case of **1**·{**2**(PF$_6$)$_2$}$_2$ and **1**·{**3**(PF$_6$)$_2$}$_2$, the E_{0-0} value for the charge transfer transition (HOMO − 1 to LUMO transition) was lower than the E_{0-0} value of **1**. This decrease is more prominent for **1**·{**2**(PF$_6$)$_2$}$_2$ than that of **1**·{**3**(PF$_6$)$_2$}$_2$ (Scheme 2), which corroborates well with the more significant spectral changes for **1**·{**2**(PF$_6$)$_2$}$_2$ than that of **1**·{**3**(PF$_6$)$_2$}$_2$. Thus, the energy levels evaluated on the basis of results of electrochemical experiments agree well with the results of the absorption and emission spectral results.

Luminescence decay profiles for the excited state were measured for **1** in presence and absence of **2**(PF$_6$)$_2$ and **3**(PF$_6$)$_2$ by time correlated single photon counting technique using 280 nm nano-LED as an excitation source (Table 2). Luminescence, monitored at 340 nm for **1**, showed a biexponential decay with τ_1 = 0.55 ns and τ_2 = 7.39 ns. A comparison of these with the emission decay lifetimes recorded for two model compounds **4** and **5** (Table 2) suggests that the contribution of the longer-lived component of the biexponential decay for **1** was due to decay of the naphthalene-based excited state in the **D1** moiety, while the shorter-lived component could be ascribed to a ICT-based excited state in the **D2** unit.

Table 2. Fluorescence Life Time Data (τ in ns) Obtained by Using 280 nm NanoLED As an Excitation Source and Monitoring Wavelength (λ_{Mon}), in Dichloromethane at 25°C[a]

host/guest	λ_{Mon} (nm)	τ (ns)	rel. (%)	χ^2
1	340	0.55, 7.59	46, 54	1.11
4	425	0.57, 2.00	87, 13	0.97
5	340	11.00	100	1.06
1{**2**(PF$_6$)$_2$}$_2$	340	0.40, 1.36, 9.46	40, 44, 16	1.23
1{**3**(PF$_6$)$_2$}$_2$	340	0.05, 1.29, 9.60	25, 12, 63	1.17
2(PF$_6$)$_2$	340	0.56, 1.53	40, 60	1.08
3(PF$_6$)$_2$	340	0.41, 5.66	56, 44	1.15

[a] χ^2 is a numerical value that reflects the overall goodness of fit (Supporting Information page 12).

The observed decrease in lifetime of both components also supports the alteration of the charge transfer-based excited states in **1**. Emission decay profiles for **1** were also recorded in

dx.doi.org/10.1021/jo300622b | J. Org. Chem. 2012, 77, 6789−6800

the presence of 2 mol equiv of $2(PF_6)_2$ and $3(PF_6)_2$. In both cases the decay profile showed a triexponential decay, suggesting the presence of three components in the excited state. The decrease of lifetime of the three components compared to their corresponding individual compound supports the presence of a lower energy charge transfer state in $1{\cdot}2(PF_6)_2$ or $1{\cdot}3(PF_6)_2$, which favors the faster deactivation according to the energy gap law.[32] This also agrees well with the electronic spectral data, which reveal that **1** forms charge transfer complexes with $2(PF_6)_2$ and $3(PF_6)_2$ and the energy of this CT transition is lower than that of **1**.

Electrochemical Study. Redox potential values for all compounds and the taco-complexes were recorded and are summarized in Table 3. Paraquat (PQ^{2+}) derivatives usually undergo two consecutive one-electron reduction processes, and both processes are chemically and electrochemically reversible.[33] The first reduction leads to the generation of a cation radical species ($PQ^{\bullet+}$) ($E_{1/2}$ = −0.39 V), and the second reduction yields the fully neutral residue (PQ) ($E_{1/2}$ = −0.80 V) species. However, the first and second reductions of the $3(PF_6)_2$ occur at less negative potentials than $2(PF_6)_2$. The presence of the benzyl substituent is expected to contribute to this observed difference. The diminished current observed for these redox processes on complexation, compared to those for individual components, confirm that the complexes have smaller diffusion coefficients. Cathodic shifts in potentials were observed for both these redox processes on complex formation, which suggests that bipyridinium unit is engaged in a charge transfer interaction with the electron donating host. As expected, the observed cathodic shift for the first reduction wave (520 mV) is larger than that of the second reduction wave (200 mV), as the CT interaction with the host molecule becomes weaker after the first reduction of the bipyridinium unit.

Table 3. Electrochemical Data for the Molecular Components Measured in Argon-Purged CH_3CN:CH_2Cl_2 Solution (1:1) at Room Temperature[a]

host/guest	oxidation (V vs SCE)	reduction (V vs SCE)
1	+1.24, +1.55[b]	
$1\{2(PF_6)_2\}_2$	+1.10, +1.91[b]	−0.91, −1.00[b]
$1\{3(PF_6)_2\}_2$	+1.03, +1.88[b]	−0.71, −0.85[b]
$2(PF_6)_2$		−0.39, −0.80[c]
$3(PF_6)_2$		−0.28, −0.69[c]
4	+1.02[c]	
5	+1.62[c]	

[a]Et_4NPF_6 was used as supporting electrolyte, and glassy carbon was used as working electrode. [b]Not fully reversible process; potential value was estimated from DPV peaks. [c]Half-wave potential values are expressed in V vs SCE for reversible and one-electron redox processes, unless otherwise indicated.

Two oxidation processes were observed for the divalent host **1** at +1.24 V and +1.55 V. A comparison of these values with those for two reference compounds **4** and **5** (Table 3) suggests that the first oxidation process at +1.24 V is due to the redox process involving the **D2** unit, while the second one at +1.55 V is associated with the **D1** unit. Thus, for the divalent host molecule **1**, the oxidation process associated with the **D2** units takes place at a potential that is 220 mV more positive than that of the corresponding reference compound **4**, and the oxidation process for **D1** unit in **1** becomes easier by 70 mV as compared to the model compound, **5**. These observations are attributed to the presence of charge transfer interactions between **D1** and **D2** units in **1**, which was also evident in the absorption spectra and reported earlier for analogous crown ethers.[34] Upon complexation of **1** with $2(PF_6)_2$ or $3(PF_6)_2$, the oxidation processes for **D1** and **D2** were found to respond differently. Appreciable anodic shifts in potential were observed for the oxidation process associated with **D1**, while cathodic shifts were evident for the **D2** fragment (Table 3), when compared with respective values for **1**. Interestingly, with this cathodic shift the oxidation potential for the **D2** fragment in $1{\cdot}\{2(PF_6)_2\}_2$ or $1{\cdot}\{3(PF_6)_2\}_2$ became comparable to that for the model compound **4** (Table 3). This observation clearly indicates that the **D1** fragment in $1{\cdot}\{2(PF_6)_2\}_2$ is involved in a new charge transfer interaction with the bipyridinium unit, while fragment **D2** in $1{\cdot}\{2(PF_6)_2\}_2$ or $1{\cdot}\{3(PF_6)_2\}_2$ is no longer under the influence of any charge transfer interaction.

Control of Reversible Complexation of 1 and $2(PF_6)_2$. Potasium ion is known to form a stable complex with dibenzo-24-crown-8 (DB24C8), and this high stability (K_a = 7.6 × 10^3 M^{-1} in acetonitrile at 25 °C) has actually helped in using K^+ as an effective templating agent for the synthesis of 24-crown-8 derivatives.[35] Literature reports also revealed that dibenzo-18-crown-6 forms a much stronger complex with the K^+ (K_a = 1.0 × 10^6 M^{-1} in CH_2Cl_2 + 2% acetonitrile at 25 °C).[36] We have used the difference in binding constants to demonstrate reversible [3](taco complex) formation as well as self-assembled phenomena for implementing logic operations based on the fluorescence response.

On addition of 8.5 mM of KPF_6 to a $CDCl_3$:CD_3CN (4:1, v/v) solution of 4.2 mM **1** and 8.5 mM $2(PF_6)_2$, an instantaneous change in the ^1H NMR spectrum was observed. Spectral shifts characteristic for the taco complex disappeared, and the original ^1H NMR spectra for $2(PF_6)_2$ was restored (Figure 7c). Significantly, a simultaneous visual change in solution color from dark brown to pale brown was observed. On further addition of 8.5 mM of KPF_6, the chemical shifts of protons of $2(PF_6)_2$ also remain the same (Figure 7d). Control experiments revealed that on addition of KPF_6, the chemical shifts of protons on $2(PF_6)_2$ remains unchanged. All these data indicate

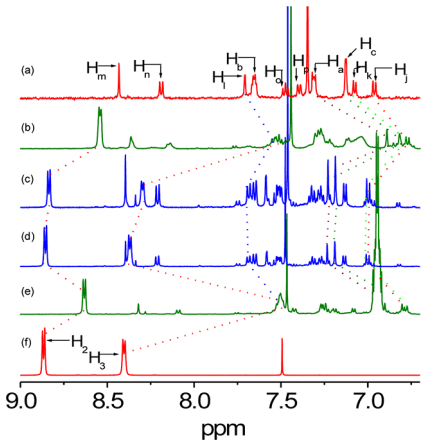

Figure 7. Partial ^1H NMR spectra (500 MHz, 298 K) recorded in $CDCl_3$:CD_3CN (4:1, v/v) for (a) 4.2 mM **1**; (b) 4.2 mM **1** with 8.5 mM $2(PF_6)_2$; (c) 4.2 mM **1** with 8.5 mM $2(PF_6)_2$ and 8.5 mM KPF_6; (d) 4.2 mM **1** with 8.5 mM $2(PF_6)_2$ and 17 mM KPF_6; (e) 4.2 mM **1** with 8.5 mM $2(PF_6)_2$, 17 mM KPF_6 and 17 mM DB18C6; (f) 8.5 mM $2(PF_6)_2$.

dx.doi.org/10.1021/jo300622b | J. Org. Chem. 2012, 77, 6789−6800

Scheme 3. Schematic Representation of the Formation of the [3](Taco Complex), Its Disassembly in Presence of K^+, and Reassembly on Subsequent Addition of DB18C6[a]

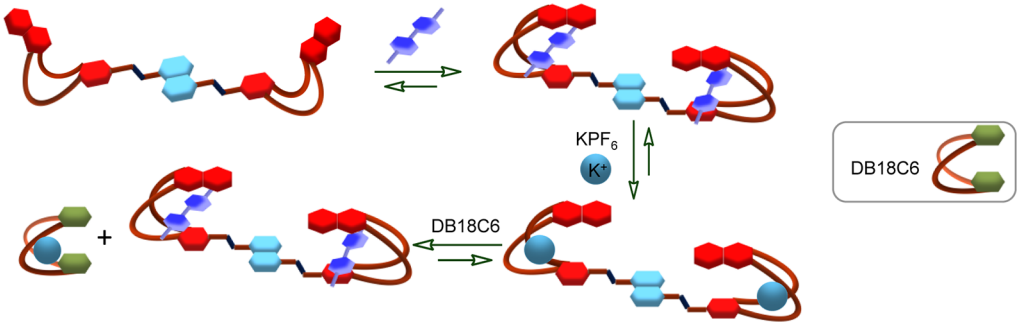

[a]The [3](taco complex) undergoes de-complexation in the presence of 2 equiv of K^+, as K^+ formed an even stronger complex with **1**. However, subsequent addition of DB18C6, which has an affinity toward K^+ even higher than that of **1**, allowed the regeneration of the complex **1**·{**2**$(PF_6)_2$}$_2$.

that complete dissociation of the taco complex, **1**·{**2**$(PF_6)_2$}$_2$, takes place in the presence of 8.5 mM KPF_6. However, upon subsequent addition of 17 mM of DB18C6 to this resultant solution, chemical shifts revert back to those for **1**·{**2**$(PF_6)_2$}$_2$ (Figure 7e), indicating the reformation of the taco complex.

Appropriate design of the host functionality and the choice of the host and guest moieties also allowed us to probe the complexation and decomplexation process for **1** and **2**$(PF_6)_2$ in the presence of other molecular inputs like KPF_6 and DB18C6 by monitoring changes in fluorescence spectral patterns (Supporting Information Figure S17).

Earlier we have shown that a significant decrease of fluorescence intensity of free **2**$(PF_6)_2$ (Φ = 0.1762, Table 1) was observed upon formation of the taco complex, **1**·{**2**$(PF_6)_2$}$_2$ (Φ = 0.0593, Table 1). On addition of 2 mol equiv of KPF_6, the fluorescence intensity at 342 nm was enhanced (Φ = 0.0821), which confirmed the decomplexation of **1**·{**2**$(PF_6)_2$}$_2$ as was also evident in the ^{1}H NMR spectra. The difference in fluorescence intensity of the solution having KPF_6 (Φ = 0.0821) with that of **2**$(PF_6)_2$ (Φ = 0.1762) was attributed to the quenching influence of the hexafluorophosphate ion[37] or crown moiety present in the solution mixture. In presence of added KPF_6, decrease of the dissociation of **2**$(PF_6)_2$ could have also contributed to this. Further, on addition of 2 equiv of DB18C6 to the solution containing (**1**·{**2**$(PF_6)_2$}$_2$ + 2 mol equiv of KPF_6), K^+ binds preferentially to DB18C6 to form K{DB18C6}$^+$ and favors the regeneration of the taco complex formation between **1** and **2**$(PF_6)_2$, and this was evident by further decrease in fluorescence intensity. Thus, the results of the fluorescence studies agree well with those obtained from ^{1}H NMR studies, and all these results demonstrated that the reversible complex formation between **1** and **2**$(PF_6)_2$ can be controlled in presence of molecular inputs like KPF_6 and DB18C6 (Scheme 3). Similar phenomena were also observed for the complexation between **1** and **3**$(PF_6)_2$ (Supporting Information Figure S16).

Logic Operations through Control of Reversibility. The results described above showed that the chemically driven reversible "taco" complex formation between **1** and **2**$(PF_6)_2$ could be achieved through sequential molecular inputs like KPF_6 and DB18C6. Three states of this process, namely, assembly (that generated **1**·{**2**$(PF_6)_2$}$_2$ on addition of **2**$(PF_6)_2$ to **1**), disassembly (that regenerated individual component **2**$(PF_6)_2$ and **1**{KPF_6}$_2$) on addition of KPF_6, and reassembly (that regenerated **1**·{**2**$(PF_6)_2$}) on addition of DB18C6, were characterized by probing distinct and specific changes in luminescence spectra. Our main focus is to demonstrate the logic operation by monitoring the optical response of **1** in presence of different inputs. By adopting appropriate threshold values and a logic convention, the physicochemical input and output signals could be used to encode binary information.[10] Monitoring the luminescence output signals at appropriate wavelengths, two basic logic operations like OR and YES could be demonstrated, while more complicated logic operations like INHIBIT gate could be demonstrated using three ionic/molecular inputs. Such behavior is rather uncommon when compared with previous reports,[26a,c,38] where mostly acid and base were used as two inputs for assembly/disassembly purposes. Here we have used three chemical input channels, e.g., DB18C6 (**In**$_1$), KPF_6 (**In**$_2$) and **2**$(PF_6)_2$ (**In**$_3$), and either one of three optical output channels (using luminescence intensity as the readout data) to describe OR, YES and INHIBIT logic operation at 310 (**Out**$_1$), 330 (**Out**$_2$), and 360 nm (**Out**$_3$), respectively. We have adopted a positive logic convention (i.e., a signal below the threshold corresponds to logic ⟨0⟩) for demonstrating these logic functions. The threshold values selected for the three output channels are indicated as the dashed lines in bar diagrams shown in Figures 8a,b and 9a. For inputs, the logic ⟨0⟩ is represented by no addition of reactant, and the logic ⟨1⟩ is represented by the addition of 2 equiv of reactant.

The output of OR gate is normally switched on in presence of either one or both inputs. To use **1** as a molecular OR gate, we used two inputs **In**$_1$ (DB18C6) and **In**$_3$ (**2**$(PF_6)_2$), and the change of luminescence intensity at 330 nm was monitored as output (**Out**$_2$). The truth table for the OR gate and the corresponding bar diagram are shown in Figure 8a.

In the absence of any of these inputs, the fluorescence intensity at 330 nm of **1** was relatively low (<2, output: ⟨0⟩), whereas the fluorescence intensities were obviously enhanced (>2, output: ⟨1⟩) in the presence of each one or both of these two inputs. As a result, a two-input OR logic gate was obtained according to the truth table shown in Figure 8a. It was also possible to construct a YES gate with **1**, by using another set of inputs (**In**$_1$ and **In**$_2$) and monitoring the fluorescence intensity at 310 nm as output (**Out**$_1$). The general feature of YES gate is to transform one input signal to output neglecting another input signal.[39] The truth table of **1** for YES gate and the corresponding bar diagram are shown in Figure 8b. The emission intensity at 310 nm for the solution of **1** in the presence of both inputs (**In**$_1$ and **In**$_2$) was relatively high (>14, output: ⟨1⟩).

dx.doi.org/10.1021/jo300622b | J. Org. Chem. 2012, 77, 6789−6800

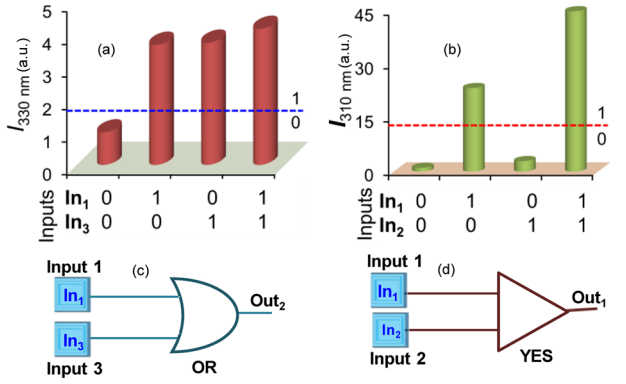

Figure 8. (a) Bar diagrams showing the experimental output values (λ_{ex} = 280 nm; **Out**$_2$, λ_{Mon} = 330 nm) for the **OR** logic states of the system, obtained on the same solution by the sequential addition of DB18C6 and **2**$(PF_6)_2$ inputs. The dashed lines mark the threshold values for the corresponding logic operations. (b) Bar diagrams showing the experimental output values (λ_{ex} = 280 nm; **Out**$_1$, λ_{Mon} = 310 nm) for the **YES** logic states of the system, obtained on the same solution by the sequential addition of DB18C6 and KPF_6 inputs. Schematic representation of (c) an **OR** logic gate (d) a **YES** logic gate.

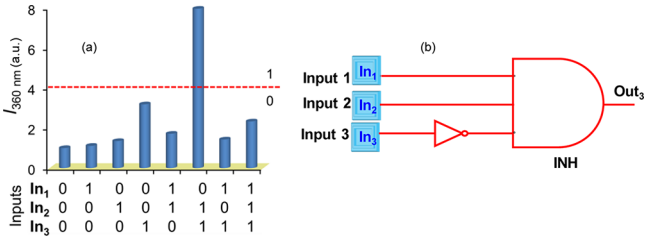

Figure 9. (a) Bar diagrams showing the experimental output values (λ_{ex} = 280 nm; **Out**$_3$, λ_{Mon} = 360 nm) for the **INHIBIT** logic states of the system, obtained on the same solution by the sequential addition of DB18C6, KPF_6 and **2**$(PF_6)_2$ inputs. The dashed lines mark the threshold values for the corresponding logic operations. (b) Schematic representation of an **INHIBIT** logic gate.

The relatively higher emission quantum yield for DB18C6 (**In**$_1$), when coordinated to K^+ of KPF_6 (**In**$_2$), contributes to the interruption of the photo induced electron transfer (PET) process associated with the crown ether moiety, whereas the fluorescence intensity of **1** is relatively low (<14, output: ⟨0⟩) in the presence and absence of **In**$_2$. Factors like flexibility and an ICT state contribute to their observed lower quantum yield. Further, emission intensity at this monitoring wavelength in the presence of the input **In**$_1$ alone was higher than the threshold value (>14, output: ⟨1⟩) due to the weak but sufficient emissive nature of DB18C6. These observations all together complied with the YES logic gate function and are presented in Figure 8b.

Until now, no example is available in the literature that demonstrates the INHIBIT logic operation by utilizing the control and reversible formation of the taco complex with three different molecular inputs. The INHIBIT logic operation with three inputs provides eight possibilities with noncommutative behavior, where one of these inputs can immobilize the whole system.[40]

By combining these three molecular inputs with eight possible input combinations, we could succeed in achieving the much more complex INHIBIT logic operation with divalent host **1**. To demonstrate this, we used three inputs (**In**$_1$, **In**$_2$ and **In**$_3$), and the luminescence intensity was monitored at 360 nm as output (**Out**$_3$). The bar diagram with corresponding truth table is presented in Figure 9a. When none of these inputs were on, the gate was off (<4, output: ⟨0⟩). Switching on happened only when one input combination (**In**$_2$ + **In**$_3$) was used and turned the gate on (>4, output: ⟨1⟩). However, use of any other input combination did not switch the gate on (<4, output: ⟨0⟩). Thus, one input combination (**In**$_2$ + **In**$_3$), out of eight possibilities could switch the gate on (Figure 9a), and thus, the observed luminescence response of divalent host **1** monitored at 360 nm met the requirements for an INHIBIT logic operation.

CONCLUSION

In summary, we have demonstrated the complexation behavior of newly synthesized divalent host **1** with two different paraquat derivatives. Detailed ^{1}H NMR study reveals that two paraquat units bind cooperatively with this host, forming a [3](taco complex). Because of preorganization of the flexible host molecule during binding, the [3](taco complex) adops a folded shape, wherein the two paraquat units are sandwiched between the two aromatic units of the folded crown ether fragment of **1**. The steady and the excited state spectra along with the results of electrochemical studies of the respective compounds and the [3](taco complexes) suggest the presence of a charge transfer state in the divalent host **1**, while on complexation with respective paraquat derivative, a new charge transfer complex is formed. The energy levels calculated on the basis of electrochemical data and E_{0-0} value for the respective molecule also agree well with spectral responses for different CT processes. We have also investigated the reversible and controlled complexation processes involving **1** and **2**$(PF_6)_2$/**3**$(PF_6)_2$ in presence of independent molecular inputs like KPF_6 and DB18C6. Preferential binding of K^+ to crown ether moieties of **1** leads to the dissociation of the [3](taco complex). Further, on subsequent addition of DB18C6 to this resulting solution, the higher affinity of DB18C6 toward K^+ allows reassembly of the [3](taco complex). These three processes, namely, assembly, disassembly, and reassembly, were probed by monitoring distinct changes in luminescence spectra associated with each process. These observed fluorescence responses at appropriate monitoring wavelengths could be used as a output signals to demonstarte in principle two basic logic gates, OR and YES, using two independent inputs (**In**$_1$ and **In**$_3$; **In**$_1$ and **In**$_2$), while an INHIBIT gate could be demonstrated in principle using three inputs. Results described in this report are expected to contribute to the development of new concepts in the field of nanoscience and to the cross-fertilization between traditionally separated disciplines such as chemistry and information science.[41]

EXPERIMENTAL SECTION

Reagents and Methods. 2,3-Dihydroxynaphthalene, 1,5-diaminonaphthalene, 2,2′,2″-chloroethoxyethoxyethanol and 3,4-dihydroxybenzaldehyde were used as received. NH_4PF_6 was recrystallized from ethanol before use. All solvents were of reagent grade, which were further dried and distilled prior to use following standard procedures. Two intermediates (**A** and **B**), which were used for synthesis of **1**, were prepared following a literature procedures.[5a] Model compound **5** was synthesized following one of our previously reported procedures.[5a] Details about various instrumentation techniques that were used for this study are provided in the Supporting Information section. Methodologies adopted for calculation of stoichiometric binding constant from ^{1}H NMR titration study and the corresponding errors in solution preparation and instrumental analysis are provided in the Supporting Information.

dx.doi.org/10.1021/jo300622b | J. Org. Chem. 2012, 77, 6789−6800

Synthesis of A. **A** was synthesized following a literature procedure, and the pure compound was isolated after purification as a sticky dark brown semisolid.[5a] Analytical and different spectroscopic data agreed well for the proposed molecular formula and the desired purity. Yield (53.0%): ^{1}H NMR (500 MHz, CD_2Cl_2, δ ppm) 7.68−7.66 (2H, m), 7.33−7.31 (2H, m), 7.15 (2H, s), 4.25 (4H, t, J = 4.5), 3.93−3.91 (4H, m), 3.74−3.73 (4H, m), 3.66−3.65 (8H, m), 3.56−3.54 (4H, m). Elemental Analysis Calcd for $C_{22}H_{32}O_8$: C, 62.25; H, 7.60. Found: C, 62.48; H, 7.53. ESI−MS calcd for $C_{22}H_{32}O_8$: 424.48. Found: 447.24 $[M + Na]^+$.

Synthesis of B. Intermediate compound **B** was synthesized, purified, and isolated as a sticky brown mass following a previously reported procedure.[5a] Yield **B** (82.0%): ^{1}H NMR (500 MHz, CD_2Cl_2, δ ppm) 7.75 (4H, d, J = 8.5), 7.66−7.65 (2H, m), 7.30 (6H, d, J = 7.5), 7.14 (2H, s), 4.20 (4H, t, J = 4.5), 4.09 (4H, t, J = 4.5), 3.85 (4H, t, J = 4.5), 3.65−3.62 (8H, m), 3.57−3.55 (4H, m), 2.36 (6H, s); ^{13}C NMR 148.9, 144.8, 132.9, 129.8, 127.8, 126.3, 124.2, 108.3, 70.7, 69.4, 68.6, 68.3, 29.6. Elemental Analysis Calcd. for $C_{36}H_{44}O_{12}S_2$: C, 59.00; H, 6.05; S, 8.75. Found: C, 59.16; H, 6.00, S, 8.70. ESI−MS Calcd. for $C_{36}H_{44}O_{12}S_2$: 732.86. Found: 755.14 $[M + Na]^+$.

Synthesis of C. 3,4-Dihydroxybenzaldehyde (0.38 g, 2.8 mmol) was dissolved in 40 mL of freshly dried DMF. To this solution K_2CO_3 powder (1.3 g, 9.6 mmol) was added. This mixture was allowed to stir for 15 min, and compound **B** (ditosylate of oligoethylene glycol derivative of naphthalene) (2.0 g, 2.7 mmol) dissolved in 50 mL of dry DMF was added in a dropwise manner over 2 h at 60 °C. Then the temperature was raised to 80 °C, and the mixture was allowed to stir for 5 days. The solvent was removed under reduced pressure; the residue was extracted three times with $CHCl_3$ and water. The organic layers were combined and dried over anhydrous sodium sulfate. Removal of the solvent under a vacuum gave crude product, which was purified on a silica gel column using $CHCl_3$:CH_3OH (98:2, v/v) to yield pure **C** (0.90 g, 62%), as a brown solid (mp 80 °C −85 °C): ^{1}H NMR (200 MHz, $CDCl_3$, δ ppm) 9.78 (1H, s), 7.64−7.63 (2H, bs); 7.38−7.35(2H, bs), 7.32−7.30 (2H, bs), 7.08 (2H, s), 6.91(1H, s), 4.25 (4H, bs), 4.22−4.20 (4H, broad m), 4.00−3.99 (4H, broad m), 3.97−3.93 (4H, broad m), 3.89−3.86 (8H, broad m); ^{13}C NMR 190.9, 162.6, 148.9, 130.1, 129.2, 126.8, 126.2, 124.2, 111.8, 110.9, 107.8, 71.5, 69.5, 69.0. Elemental Analysis Calcd for $C_{29}H_{34}O_9$: C, 66.15; H, 6.51. Found: C, 65.93; H, 6.48. ESI−MS Calcd for $C_{29}H_{34}O_9$: 526.22. Found: 549.39 $[M + Na]^+$.

Synthesis of 1. Compound **C** (0.2 g, 0.4 mmol) was dissolved in 20 mL of dry methanol. To this solution 0.03 g (0.2 mmol) of 1,5-diaminonaphthalene was added. Then the reaction mixture was stirred for 2 days at room temperature. After 2 days a dark green precipitate appeared, which was filtered through a G3 crucible and washed 3−4 times with cold methanol. Then the product was dried in vacuum to isolate the desired product as a dark green solid (mp 175 °C −180 °C). Yield (0.16 g, 80%): ^{1}H NMR (500 MHz, $CDCl_3$, δ ppm) 8.43 (2H, s), 8.19 (2H, d, J = 8.5); 7.70 (2H, s); 7.66 (4H, m); 7.47 (2H, t, J = 7.5); 7.40 (2H, d, J = 8.5); 7.31 (4H, m); 7.12 (4H, s); 7.08 (2H, d, J = 7); 6.97 (2H, d, J = 8.5); 4.30 (4H, t, J = 4); 4.27 (8H, t, J = 2); 4.24 (4H, t, J = 4); 4.00 (8H, t, J = 4); 3.97 (8H, s); 3.88 (16H, s); ^{13}C NMR 159.6, 149.2, 130.3, 129.9, 126.2, 125.7, 124.4, 121.5, 113.3, 112.6, 111.6, 106.0, 71.4, 69.7, 69.5. HRMS spectrum calculated for $C_{68}H_{74}N_2O_{16}$: 1175.5117. Found: 1175.5026.

Synthesis of 4. 3,4-Dimethoxybenzaldehyde (0.48 g, 2.9 mmol) was dissolved in 20 mL of dry methanol, and a solution (0.2 g, 1 mmol) of 1,5-diaminonaphthalene was added. The reaction mixture was stirred for 2 days at room temperature. After 2 days a dark green precipitate appeared, which was filtered through a G3 crucible and washed 3−4 times with cold ethanol. Then the product was dried in vacuum. Yield (0.45 g, 80.0%), as a dark color solid (mp 230−235 °C): ^{1}H NMR (500 MHz, $CDCl_3$, δ ppm) 8.47 (2H, s), 8.21 (2H, d, J = 8.5); 7.77 (2H, bs); 7.49 (2H, t, J = 7.5); 7.41 (2H, dd, J = 2, 8); 7.09 (2H, d, J = 7.5); 6.98 (2H, d, J = 8.0); 4.03 (6H, s); 3.98 (6H, s). Elemental Analysis Calcd for $C_{28}H_{26}N_2O_4$: C, 73.99; H, 5.77; N, 6.16;. Found: C, 73.75; H, 5.74; N, 6.13. (ESI−MS) calcd for $C_{28}H_{26}N_2O_4$: 454.19. Found: 455.43 $[M + H]^+$.

Synthesis of 5. Model compound **5** was prepared and isolated as a white powder (mp 90 °C) following a previously reported procedure.[5a] Yield **5** (63.0%): ^{1}H NMR (500 MHz, $CDCl_3$, δ ppm) 7.65−7.63 (2H, m), 7.32−7.30 (2H, m), 7.09 (2H, s), 6.89−6.84 (4H, m), 4.25 (4H, t, J = 4), 4.15 (4H, t, J = 4), 3.98 (4H, t, J = 4), 3.93 (4H, t, J = 4), 3.89−3.85 (8H, m); ^{13}C NMR 150.9, 131.1, 128.0, 125.9, 123.2, 116.1, 109.7, 73.1, 71.9, 71.1. Elemental Analysis Calcd for $C_{28}H_{34}O_8$: C, 67.45; H, 6.87. Found: C, 67.32; H, 6.84. (ESI−MS) Calcd for $C_{28}H_{34}O_8$: 498.56. Found: 521.58 $[M + Na]^+$.

■ ASSOCIATED CONTENT

Ⓢ Supporting Information

Details about general instrumentation techniques, ^{1}H NMR, ^{13}C NMR, and ESI-Mass spectra, 2D-COSY spectra for **1**·{**2**$(PF_6)_2$}$_2$ and **1**·{**3**$(PF_6)_2$}$_2$. Detailed spectroscopic results (UV−vis, Fluorescence) and cyclic voltammograms. Details of determination of binding constants, methods of error calculation, methods of determining energy levels. This material is available free of charge via the Internet at http://pubs.acs.org.

■ AUTHOR INFORMATION

Corresponding Author

*E-mail: amitava@csmcri.org.

Notes

The authors declare no competing financial interest.

■ ACKNOWLEDGMENTS

A.D. thanks DST (India) and CSIR (India) for financial support to this research. A.K.M., P.D., and P.M. acknowledge CSIR for their research fellowship. S.A. acknowledges Indian Academy of Sciences for supporting his stay at CSMCRI under the Summer Fellowship Programme.

■ REFERENCES

(1) (a) Harada, A. *Acc. Chem. Res.* **2001**, *34*, 456−464. (b) Schalley, C. A.; Beizai, K.; Vögtle, F. *Acc. Chem. Res.* **2001**, *34*, 465−476. (c) Ballardini, R.; Balzani, V.; Credi, A.; Gandolfi, M. T.; Venturi, M. *Acc. Chem. Res.* **2001**, *34*, 445−455. (d) Felder, T.; Schalley, C. A. *Angew. Chem., Int. Ed.* **2003**, *42*, 2258−2260. (e) Onagi, H.; Blake, C. J.; Easton, C. J.; Lincoln, S. F. *Chem.—Eur. J.* **2003**, *9*, 5978−5988. (f) Badjic, J. D.; Balzani, V.; Credi, A.; Silvi, S.; Stoddart, J. F. *Science* **2004**, *303*, 1845−1849. (g) Hernandez, J. V.; Kay, E. R.; Leigh, D. A. *Science* **2004**, *306*, 1532−1537. (h) Scarso, A.; Onagi, H.; Rebek, J, Jr. *J. Am. Chem. Soc.* **2004**, *126*, 12728−12729.

(2) (a) Ashton, P. R.; Baxter, I.; Fyfe, M. C. T.; Raymo, F. M.; Spencer, N.; Stoddart, J. F.; White, A. J. P.; Williams, D. J. *J. Am. Chem. Soc.* **1998**, *120*, 2297−2307. (b) Pease, A. R.; Jeppesen, J. O.; Stoddart, J. F.; Luo, Y.; Collier, C. P.; Heath, J. R. *Acc. Chem. Res.* **2001**, *34*, 433−444. (c) Gibson, H. W.; Ge, Z.; Jones, J. W.; Harich, K.; Pederson, A.; Dorn, H. C. *J. Polym. Sci., Part A: Polym. Chem.* **2009**, *47*, 6472−6495. (d) Gibson, H. W.; Yamaguchi, N.; Niu, Z.; Jones, J. W.; Slebodnick, C.; Rheingold, A. L.; Zakharov, L. N. *J. Polym. Sci., Part A: Polym. Chem.* **2010**, *48*, 975−985. (e) Hmadeh, M.; Fang, L.; Trabolsi, A.; Elhabiri, M.; Gary, A. M. A.; Stoddart., J. F. *J. Mater. Chem.* **2010**, *20*, 3422−3430. (f) Gibson, H. W.; Jones, L. W.; Zakharov, L. N.; Rheingold, A. L.; Slebodnick, C. *Chem.—Eur. J.* **2011**, *17*, 3192−3206. (g) Dey, S. K.; Beuerle, F.; Olson, M. A.; Stoddart., J. F. *Chem. Commun.* **2011**, *47*, 1425−1427. (h) Huang, F.; Gibson, H. W.; Bryant, W. S.; Nagvekar, D. S.; Fronczek, F. R. *Org. Lett.* **2012**, *14*, 306−309. (i) Forgan, R. S.; Wang, C.; Friedman, D. C.; Spruell, J. M.; Stern, C. L.; Sarjeant, A. A.; Cao, D.; Stoddart, J. F. *Chem.—Eur. J.* **2012**, *18*, 202−212.

(3) (a) Anelli, P. L.; Ashton, P. R.; Ballardini, R.; Balzani, V.; Delgado, M.; Gandolfi, M. T.; Goodnow, T. T.; Kaifer, A. E.; Philp, D.; Pietraszkiewicz, M.; Prodi, L.; Reddington, M. V.; Slawin, A. M. Z.; Spencer, N.; Stoddart, J. F.; Vicent, C.; Williams, D. J. *J. Am. Chem.*

Soc. **1992**, *114*, 193−219. (b) Gong, C.; Gibson, H. W. *Angew. Chem., Int. Ed.* **1998**, *37*, 310−314. (c) Niu, Z.; Gibson, H. W. *Chem. Rev.* **2009**, *109*, 6024−6046. (d) Niu, Z.; Huang, F.; Gibson, H. W. *J. Am. Chem. Soc.* **2011**, *133*, 2836−2839. (e) Barin, G.; Coskun, A.; Fouda, M. M. G.; Stoddart, J. F. *ChemPlusChem* **2012**, *77*, 159−185. (f) Zheng, B.; Wang, F.; Dong, S.; Huang, F. *Chem. Soc. Rev.* **2012**, *41*, 1621−1636.

(4) (a) Yamaguchi, N.; Gibson, H. W. *Angew. Chem., Int. Ed.* **1999**, *38*, 143−147. (b) Klivansky, L. M.; Koshkakaryan, G.; Cao, D.; Liu, Y. *Angew. Chem., Int. Ed.* **2009**, *48*, 4185−4189. (c) Li, S.; Liu, M.; Zheng, B.; Zhu, K.; Wang, F.; Li, N.; Zhao, X.-L.; Huang, F. *Org. Lett.* **2009**, *11*, 3350−3353. (d) Zhang, M.; Zhu, K.; Huang, F. *Chem. Commun.* **2010**, *46*, 8131−8141. (e) Niu, Z.; Huang, F.; Gibson, H. W. *J. Am. Chem. Soc.* **2011**, *133*, 133−136. (f) Niu, Z.; Slebodnick, C.; Bonrad, K.; Huang, F.; Gibson., H. W. *Org. Lett.* **2011**, *13*, 2872−2875. (g) Niu, Z.; Slebodnick, C.; Huang, F.; Azurmendi, H.; Gibson, H. W. *Tetrahedron Lett.* **2011**, *52*, 6379−6382. (h) Niu, Z.; Slebodnick, C.; Schoonover, D.; Azurmendi, H.; Harich, K.; Gibson, H. W. *Org. Lett.* **2011**, *13*, 3992−3995. (i) Niu, Z.; Slebodnick, C.; Gibson, H. W. *Org. Lett.* **2011**, *13*, 4616−4619. (j) Yan, X.; Zhang, M.; Wei, P.; Zheng, B.; Chi, X.; Ji, X.; Huang, F. *Chem. Commun.* **2011**, *47*, 9840−9842.

(5) (a) Suresh, M.; Mandal, A. K.; Kesharwani, M. K.; Adarsh, N. N.; Ganguly, B.; Kanaparthi, R. K.; Samanta, A.; Das, A. *J. Org. Chem.* **2011**, *76*, 138−144. (b) Mandal, A. K.; Suresh, M.; Das, A. *Org. Biomol. Chem.* **2011**, *9*, 4811−4817.

(6) (a) Allwood, B. L.; Spencer, N.; Sharhriari-Zavareh, H.; Stoddart, J. F.; Williams, D. J. *J. Chem. Soc., Chem. Commun.* **1987**, 1058−1061. (b) 1064−1066. (c) Stoddart, F. *Chem. Ber.* **1991**, 714−718.

(7) Ashton, P. R.; Fyfe, M. C. T.; Martinez-Diaz, M. V.; Menzer, S.; Schiavo, C.; Stoddart, J. F.; White, A. J. P.; Williams, D. J. *Chem.—Eur. J.* **1998**, *4*, 1523−1534.

(8) (a) Bryant, W. S.; Jones, J. W.; Mason, P. E.; Guzei, I. A.; Rheingold, A. L.; Nagvekar, D. S.; Gibson, H. W. *Org. Lett.* **1999**, *1*, 1001−1004. (b) Jones, J. W.; Zakharov, L. N.; Rheingold, A. L.; Gibson, H. W. *J. Am. Chem. Soc.* **2002**, *124*, 13378−13379. (c) Huang, F.; Fronczek, F. R.; Gibson, H. W. *Chem. Commun.* **2003**, 1480−1481. (d) Huang, F.; Lam, M.; Mahan, E. J.; Rheingold, A. L.; Gibson, H. W. *Chem. Commun.* **2005**, 3268−3270.

(9) Huang, F.; Switek, K. A.; Zakharov, L. N.; Fronczek, F. R.; Slebodnick, C.; Lam, M.; Golen, J. A.; Bryant, W. S.; Mason, P.; Rheingold, A. L.; Ashraf- Khorassani, M.; Gibson, H. W. *J. Org. Chem.* **2005**, *70*, 3231−3241.

(10) (a) de Silva, A. P.; Gunaratne, H. Q. N.; Gunnlaugsson, T.; Huxley, A. J. M.; McCoy, C. P.; Rademacher, J. T.; Rice, T. E. *Chem. Rev.* **1997**, *97*, 1515−1566. (b) Raymo, F. M. *Adv. Mater.* **2002**, *14*, 401−414. (c) Balzani, V.; Credi, A.; Venturi, M. *ChemPhysChem.* **2003**, *4*, 49−59. (d) Pischel, U. *Angew. Chem., Int. Ed.* **2007**, *46*, 4026−4040. (e) Szaciłowski, K. *Chem. Rev.* **2008**, *108*, 3481−3548. (f) Amelia, M.; Zou, L.; Credi, A. *Coord. Chem. Rev.* **2010**, *254*, 2267−2280.

(11) de Silva, A. P.; Gunaratne, H. Q. N.; McCoy, C. P. *Nature* **1993**, *364*, 42−44.

(12) (a) de Silva, A. P.; Gunaratne, H. Q. N.; McCoy, C. P. *J. Am. Chem. Soc.* **1997**, *119*, 7891−7892. (b) Stojanovic, M. N.; Mitchell, T. E.; Stefanovic, D. *J. Am. Chem. Soc.* **2002**, *124*, 3555−3561. (c) Delgado, J. L.; Cruz, P. D.; Lpez-Arza, V.; Langa, F.; Kimball, D. B.; Haley, M. M.; Araki, Y.; Ito, O. *J. Org. Chem.* **2004**, *69*, 2661−2668. (d) Uchiyama, S.; Kawai, N.; de Silva, A. P.; Iwai, K. *J. Am. Chem. Soc.* **2004**, *126*, 3032−3033. (e) Zhou, Y. C.; Zhang, D. Q.; Zhang, Y. Z.; Tang, Y. L.; Zhu, D. B. *J. Org. Chem.* **2005**, *70*, 6164−6170.

(13) (a) Ghosh, P.; Bharadwaj, P. K. *J. Am. Chem. Soc.* **1996**, *118*, 1553−1554. (b) De, S.; Pal, A.; Pal, T. *Langmuir* **2000**, *16*, 6855−6861.

(14) (a) Baytekin, H. T.; Akkaya, E. U. *Org. Lett.* **2000**, *2*, 1725−1727.

(15) (a) de Silva, A. P.; Dixon, I. M.; Gunaratne, H. Q. N.; Gunnlaugsson, T.; Maxwell, P. R. S.; Rice, T. E. *J. Am. Chem. Soc.* **1999**, *121*, 1393−1394. (b) Gunnlaugsson, T.; MacDonaill, D. A.; Parker, D. *Chem. Commun.* **2000**, 93−94. (c) Gunnlaugsson, T.; MacDonaill, D. A.; Parker, D. *J. Am. Chem. Soc.* **2001**, *123*, 12866−12876. (d) de-Sousa, M.; de Castro, B.; Abad, S.; Miranda, M. A.; Pischel, U. *Chem. Commun.* **2006**, 2051−2053.

(16) (a) Turfan, B.; Akkaya, E. U. *Org. Lett.* **2002**, *4*, 2857−2859. (b) Wang, Z.; Zheng, G.; Lu, P. *Org. Lett.* **2005**, *7*, 3669−3672. (c) Kumar, M.; Kumar, R.; Bhalla, V. *Org. Lett.* **2011**, *13*, 366−369.

(17) (a) Balzani, V.; Credi, A.; Venturi, M. *Coord. Chem. Rev.* **1998**, *171*, 3−16. (b) Pina, F.; Melo, M. J.; Maestri, M.; Passaniti, P.; Balzani, V. *J. Am. Chem. Soc.* **2000**, *122*, 4496−4498. (c) de Silva, A. P.; McClenaghan, N. D. *Chem.—Eur. J.* **2002**, *8*, 4935−4945. (d) Bergamini, G.; Saudan, C.; Ceroni, P.; Maestri, M.; Balzani, V.; Gorka, M.; Lee, S.-K.; van Heyst, J.; Vögtle, F. *J. Am. Chem. Soc.* **2004**, *126*, 16466−16471.

(18) (a) Asakawa, M.; Ashton, P. R.; Balzani, V.; Credi, A.; Mattersteig, G.; Matthews, O. A.; Montalti, M.; Spencer, N.; Stoddart, J. F.; Venturi, M. *Chem.—Eur. J.* **1997**, *3*, 1992−1996. (b) Lee, S. H.; Kim, J. Y.; Kim, S. K.; Leed, J. H.; Kim, J. S. *Tetrahedron* **2004**, *60*, 5171−5176.

(19) (a) de Silva, A. P.; McClenaghan, N. D. *J. Am. Chem. Soc.* **2000**, *122*, 3965−3966. (b) Remacle, F.; Speiser, S.; Levine, R. D. *J. Phys. Chem. B* **2001**, *105*, 5589−5591. (c) Stojanoviae, M. N.; Stefanovia, D. *J. Am. Chem. Soc.* **2003**, *125*, 6673−6676. (d) Andréasson, J.; Kodis, G.; Terazono, Y.; Liddell, P. A.; Bandyopadhyay, S.; Mitchell, R. H.; Moore, T. A.; Moore, A. L.; Gust, D. *J. Am. Chem. Soc.* **2004**, *126*, 15926−15927. (e) Guo, X. F.; Zhang, D. Q.; Zhang, G. X.; Zhu, D. B. *J. Phys. Chem. B* **2004**, *108*, 11942−11945. (f) Qu, D. H.; Wang, Q. C.; Tian, H. *Angew. Chem., Int. Ed.* **2005**, *44*, 5296−5299. (g) Andréasson, J.; Straight, S. D.; Kodis, G.; Park, C. D.; Hambourger, M.; Gervaldo, M.; Albinsson, B.; Moore, T. A.; Moore, A. L.; Gust, D. *J. Am. Chem. Soc.* **2006**, *128*, 16259−16265. (h) Zhou, Y. C.; Wu, H.; Qu, L.; Zhang, D. Q.; Zhu, D. B. *J. Phys. Chem. B* **2006**, *110*, 15676−15679.

(20) (a) Langford, S. J.; Yann, T. *J. Am. Chem. Soc.* **2003**, *125*, 11198−11199. (b) Coskun, A.; Deniz, E.; Akkaya, E. U. *Org. Lett.* **2005**, *7*, 5187−5189. (c) Suresh, M.; Jose, D. A.; Das, A. *Org. Lett.* **2007**, *9*, 441−444. (d) Luxami, V.; Kumar, S. *New J. Chem.* **2008**, *32*, 2074−2079. (e) Zong, G. Q.; Lu, G. X. *J. Phys. Chem. C* **2009**, *113*, 2541−2546.

(21) (a) Pischel, U.; Heller, B. *New J. Chem.* **2008**, *32*, 395−400. (b) Guo, Z. Q.; Zhao, P.; Zhu, W. H.; Huang, X. M.; Xie, Y. S.; Tian, H. *J. Phys. Chem. C* **2008**, *112*, 7047−7053.

(22) (a) Andréasson, J.; Straight, S. D.; Bandyopadhyay, S.; Mitchell, R. H.; Moore, T. A.; Moore, A. L.; Gust, D. *Angew. Chem., Int. Ed.* **2007**, *46*, 958−961. (b) Amelia, M.; Baroncini, M.; Credi, A. *Angew. Chem., Int. Ed.* **2008**, *47*, 6240−6243.

(23) For some examples on interconnection between logic gates, see: (a) Raymo, F. M.; Giordani, S. *Org. Lett.* **2001**, *3*, 3475−3478. (b) Raymo, F. M.; Giordani, S. *Org. Lett.* **2001**, *3*, 1833−1836. (c) Raymo, F. M.; Giordani, S. *J. Am. Chem. Soc.* **2002**, *124*, 2004−2007. (d) Guo, X. F.; Zhang, D. Q.; Tao, H. R.; Zhu, D. B. *Org. Lett.* **2004**, *6*, 2491−2494. (e) Silvi, S.; Constable, E. C.; Housecroft, C. E.; Beves, J. E.; Dunphy, E. L.; Tomasulo, M.; Raymo, F. M.; Credi, A. *Chem.—Eur. J.* **2009**, *15*, 178−185.

(24) (a) Whitesides, G. M.; Mathias, J. P.; Seto, C. T. *Science* **1991**, *254*, 1312−1319. (b) Philp, D.; Stoddart, J. F. *Angew. Chem., Int. Ed. Engl.* **1996**, *35*, 1154−1196. (c) Whitesides, G. M.; Grzybowski, B. *Science* **2002**, *295*, 2418−2421. (d) Lehn, J.-M. *Science* **2002**, *295*, 2400−2403. (e) Lehn, J.-M. *Proc. Natl. Acad. Sci. U.S.A.* **2002**, *99*, 4763−4768.

(25) (a) Wu, A.; Isaacs, L. *J. Am. Chem. Soc.* **2003**, *125*, 4831−4835. (b) Mukhopadhyay, P.; Wu, A.; Isaacs, L. *J. Org. Chem.* **2004**, *69*, 6157−6164. (c) Mukhopadhyay, P.; Zavalij, P. Y.; Isaacs, L. *J. Am. Chem. Soc.* **2006**, *128*, 14093−14102. (d) Jiang, W.; Winkler, H. D. F.; Schalley, C. A. *J. Am. Chem. Soc.* **2008**, *130*, 13852−13853. (e) Jiang, W.; Schalley, C. A. *Proc. Natl. Acad. Sci. U.S.A.* **2009**, *106*, 10425−10429.

(26) (a) Balzani, V.; Credi, A.; Langford, S. J.; Stoddart, J. F. *J. Am. Chem. Soc.* **1997**, *119*, 2679−2681. (b) Jiang, W.; Han, M.; Zhang, H. Y.; Zhang, Z. J.; Liu, Y. *Chem.—Eur. J.* **2009**, *15*, 9938−9945. (c) Semeraro, M.; Credi, A. *J. Phys. Chem. C* **2010**, *114*, 3209−3214.

(27) Huang, F.; Gantzel, P.; Nagvekar, D. S.; Rheingold, A. L.; Gibson, H. W. *Tetrahedron Lett.* **2006**, *47*, 7841−7844.
(28) Huang, F.; Jones, J. W.; Slebodnick, C.; Gibson, H. W. *J. Am. Chem. Soc.* **2003**, *125*, 14458−14464.
(29) Ashton, P. R.; Langford, S. J.; Spencer, N.; Stoddart, J. F.; White, A. J. P.; Williams, D. J. *Chem. Commun.* **1996**, 1387−1388.
(30) (a) Peng, X. X.; Lu, H. Y.; Han, T.; Chen, C. F. *Org. Lett.* **2007**, *9*, 895−898. (b) Cao, J.; Lu, H. Y.; You, X. J.; Zheng, Q. Y.; Chen, C. F. *Org. Lett.* **2009**, *11*, 4446−4449.
(31) (a) Marshall, A. G. *Biophysical Chemistry*; Wiley and Sons: New York, 1978; pp 70−77. (b) Hayman, B. P. *Acc. Chem. Res.* **1986**, *19*, 90−96. (c) Connors, K. A. *Binding Constants*; Wiley and Sons: New York, 1987; pp 78−86. (d) Gibson, H. W.; Yamaguchi, N.; Hamilton, L.; Jones, J. W. *J. Am. Chem. Soc.* **2002**, *124*, 4653−4665. (e) Huang, F.; Jones, J. W.; Gibson, H. W. *J. Org. Chem.* **2007**, *72*, 6573−6576. (f) Huang, F.; Fronczek, F. R.; Gibson, H. W. *J. Am. Chem. Soc.* **2003**, *125*, 9272−9273. (g) Niu, Z.; Gibson, H. W. *Org. Biomol. Chem.* **2011**, *9*, 6909−6912.
(32) (a) Droumaguet, C. L.; Mongin, O.; Werts, M. H. V.; Blanchard-Desce, M. *Chem. Commun.* **2005**, 2802−2804. (b) Woo, H. Y.; Liu, B.; Kohler, B.; Korystov, D.; Mikhailovsky, A.; Bazan, G. C. *J. Am. Chem. Soc.* **2005**, *127*, 14721−14729.
(33) Monk, P. *The Viologens: Physicochemical Properties, Synthesis and Applications of the Salts of 4, 4/-Bipyridine*; Wiley: New York, 1998; Chapter 9.
(34) Balzani, V.; Credi, A.; Mattersteig, G.; Matthews, O. A.; Raymo, F. M.; Stoddart, J. F.; Venturi, M.; White, A. J. P.; Williams, D. J. *J. Org. Chem.* **2000**, *65*, 1924−1936 and references therein.
(35) (a) Takeda, Y. *Bull. Chem. Soc. Jpn.* **1983**, *56*, 3600−3602. (b) Takeda, Y.; Kudo, Y.; Fujiwara, S. *Bull. Chem. Soc. Jpn.* **1985**, *58*, 1315−1316. (c) Gibson, H. W.; Wang, H.; Slebodnick, C.; Merola, J.; Kassel, W. S.; Rheingold, A. L. *J. Org. Chem.* **2007**, *72*, 3381−3393. (d) He, C.; Shi, Z.; Zhou, Q.; Li, S.; Li, N.; Huang, F. *J. Org. Chem.* **2008**, *73*, 5872−5880. (e) Ding, Z. J.; Zhang, Y. M.; Teng, X.; Liu, Y. *J. Org. Chem.* **2011**, *76*, 1910−1913.
(36) Chaikovskaya, A. A.; Kudrya, T. N.; Tochilkina, L. M.; Pinchuk, A. M. *Russ. J. Gen. Chem.* **1988**, *58*, 1127−1130.
(37) Peon, J.; Tan, X.; Hoerner, J. D.; Xia, C.; Luk, Y. F.; Kohler, B. *J. Phys. Chem. A* **2001**, *105*, 5768−5777.
(38) (a) Shlyahovsky, B.; Li, Y.; Lioubashevski, O.; Elbaz, J.; Willner, I. *ACS Nano* **2009**, *3*, 1831−1843. (b) Liu, D.; Chen, W.; Sun, K.; Deng, W.; Zhang, Z.; Jiang, X. *Angew. Chem., Int. Ed.* **2011**, *50*, 4103−4107. (c) Wang, H.; Wu, H.; Xue, L.; Shi, Y.; Li, X. *Org. Biomol. Chem.* **2011**, *9*, 5436−5444.
(39) Szacilowski, K.; Macyk, W.; Stochel, G. *J. Am. Chem. Soc.* **2006**, *128*, 4550−4551.
(40) Balzani, V.; Venturi, M.; Credi, A. *Molecular Devices and Machines: A Journey into the Nanoworld*; Wiley-VCH: Weinheim, 2003.
(41) Credi, A.; Garavelli, M.; Laneve, C.; Pradalier, S.; Silvi, S.; Zavattaro, G. *Theor. Comput. Sci.* **2008**, *408*, 17−30.